nature research

https://doi.org/10.1038/s41567-020-01111-0

Supplementary information

Clocking Auger electrons

In the format provided by the authors and unedited

Clocking Auger electrons: Supplementary information

D. C. Haynes[1,2,3], M. Wurzer[4], A. Schletter[4], A. Al-Haddad[5,6], C. Blaga[7,8], C. Bostedt[5,6,9], J. Bozek[10], H. Bromberger[2,11], M. Bucher[6], A. Camper[7], S. Carron[12], R. Coffee[12], J. T. Costello[13], L. F. DiMauro[7], Y. Ding[12], K. Ferguson[12], I. Grguraš[1,2], W. Helml[4,14], M. C. Hoffmann[12], M. Ilchen[15,16], S. Jalas[17], N. M. Kabachnik[15,18], A. K. Kazansky[19], R. Kienberger[4], A. R. Maier[2,17], T. Maxwell[12], T. Mazza[15], M. Meyer[15], H. Park[7], J. Robinson[12], C. Roedig[7], H. Schlarb[11], R. Singla[1,2], F. Tellkamp[1,2], P. A. Walker[2,17], K. Zhang[7], G. Doumy[6], C. Behrens[11], A. L. Cavalieri[1,2,3,5,20]

[1] *Max Planck Institute for the Structure and Dynamics of Matter, Luruper Chausee 149, 22761 Hamburg, Germany*
[2] *Center for Free-Electron Laser Science, Luruper Chaussee 149, 22761 Hamburg, Germany*
[3] *The Hamburg Centre for Ultrafast Imaging, Universität Hamburg, Mittelweg 177, 20148 Hamburg, Germany*
[4] *Physics Department, Technische Universität München, James Franck Straße, 85748 Garching, Germany*
[5] *Paul Scherrer Institute, Forschungsstrasse 111, 5232 Villigen, Switzerland*
[6] *Chemical Sciences and Engineering Division, Argonne National Laboratory, 9700 S. Cass Avenue, Lemont, IL, 60439, USA*
[7] *The Ohio State University, Columbus, OH 43210, USA*
[8] *Kansas State University, Manhattan, KS 66506, USA*
[9] *LUXS Laboratory for Ultrafast X-ray Sciences, Institute of Chemical Sciences and Engineering, Ecole Polytechnique Fédérale de Lausanne (EPFL), CH-1015 Lausanne, Switzerland*
[10] *Synchrotron SOLEIL, l'Orme des Merisiers, Saint-Aubin, BP 48, 91192 Gif-sur-Yvette, France*
[11] *Deutsches Elektronen-Synchrotron, Notkestraße 85, 22607 Hamburg, Germany*
[12] *Linac Coherent Light Source/SLAC National Accelerator Laboratory, 2575 Sand Hill Rd, Menlo Park, CA 94025, USA*
[13] *National Center for Plasma Science and Technology and School of Physical Sciences, Dublin City University, Dublin, Ireland*
[14] *Technische Universität Dortmund, Maria-Goeppert-Mayer-Straße 2, 44227 Dortmund, Germany*
[15] *European XFEL GmbH, Holzkoppel 4, 22869 Schenefeld, Germany*
[16] *Institut für Physik und CINSaT, Universität Kassel, Heinrich-Plett-Str. 40, 34132 Kassel, Germany*
[17] *Department of Physics, Universität Hamburg, Luruper Chaussee 149, 22761 Hamburg, Germany*
[18] *Skobeltsyn Institute of Nuclear Physics, Lomonosov Moscow State University, Moscow 119991, Russia*
[19] *Departamento de Fisica de Materiales, University of the Basque Country UPV/EHU; Donostia International Physics Center (DIPC), E-20019 San Sebastian/Donostia, Basque Country; IKERBASQUE, Basque Foundation for Science, E-48011 Bilbao, Spain*
[20] *Institute of Applied Physics, University of Bern, Sidlerstr. 5, 3012 Bern, Switzerland*

Correspondence and requests for materials should be addressed to D.C.H. (email: daniel.haynes@mpsd.mpg.de) or A.L.C. (email: adrian.cavalieri@iap.unibe.ch).

S1: Theoretical background to the experimental method

In order to identify the Auger decay lifetime from our measurement of the delay between photo- and Auger emission, we performed a quantum-mechanical simulation of electron streaking for both photo- and Auger electrons. In this mathematical treatment of our experiment, we will consider the photoionisation of the neon 1s shell by a few-femtosecond, linearly polarised X-ray pulse. Photo- and Auger emission occur in the presence of a linearly polarised infrared (IR) field, synchronised with the ionising FEL pulse. It is assumed that the two beams are collinear and polarised along the z-direction.

The photo- and Auger electrons are not detected in coincidence, so they may be considered as propagating independently. Since both types of electrons are relatively fast ($E_{el} > 1$ a.u.), one can apply the Strong Field Approximation (SFA) [1, 2], wherein the probability of emission of a photoelectron with momentum $\vec{k}$ can be written as

$$W_{ph}(\vec{k}) = C \left| \int_{-\infty}^{\infty} dt \, \widetilde{\varepsilon_X(t)} \, D_{\vec{k}} \exp\left[i\Phi_{ph}(\vec{k}, t) \right] \right|^2 . \tag{1}$$

Here and in the following, all quantities are given in atomic units, unless otherwise stated. In equation (1), $\widetilde{\varepsilon_X(t)}$ is the envelope of the X-ray pulse, $D_{\vec{k}}$ is the dipole matrix element describing the transition of the electron from the ground state to the continuum, C is a constant which does not affect the following discussion, and $\Phi_{ph}(\vec{k}, t)$ is related to the Volkov phase accumulated by the photoelectron as it moves in the IR field [3]. This can be written as

$$\Phi_{ph}(\vec{k}, t) = -\int_{t}^{\infty} dt' \left[\frac{1}{2} \left(\vec{k} - \overrightarrow{A_{IR}}(t') \right)^2 + (E_b - \omega_X) \right], \tag{2}$$

where E_b is the absolute value of the photoelectron binding energy and ω_x is the carrier frequency of the X-ray pulse, so that the energy of the photoelectron in the absence of the IR pulse E_{ph} is given by $E_{ph} = \omega_X - E_b$. $\overrightarrow{A_{IR}}(t)$ is the vector potential of the IR laser field with electric field vector $\overrightarrow{\varepsilon_{IR}}(t) = \overrightarrow{\varepsilon_0} \cos(\omega_{IR} t)$, such that

$$\overrightarrow{A_{IR}}(t) = -\int_{t}^{\infty} dt' \overrightarrow{\varepsilon_{IR}}(t'). \tag{3}$$

Analogous to equation (1), we can calculate the probability of emission of an Auger electron of momentum $\vec{k}$ within the SFA [4]:

$$W_A(\vec{k}) = \frac{\Gamma}{8\pi}\left|\int_{t_0}^{\infty} dt \exp\left[i\Phi_A(t) - \frac{\Gamma(\mathrm{t}-\mathrm{t}_0)}{2}\right] * \int_{t_0}^{t} dt' \widetilde{\varepsilon_X(t')}\, D_{\vec{k}} \exp\left[i\left(\left(E_e - \frac{i\Gamma}{2}\right)(t'-t_0) - (\omega_X - E_b)t'\right)\right]\right|^2. \quad (4)$$

Here, t_0 is the moment the X-ray pulse starts to interact with the system, E_e is the energy of the correlated photoelectron, and Γ is the width of the Auger state, obtained from the Auger lifetime τ_A by the relation $\tau_A = \frac{1}{\Gamma}$. The quantity $\Phi_A(t)$ is defined as

$$\Phi_A(t) = -\int_t^{\infty} dt' \left[\frac{1}{2}\left(\vec{k} - \overrightarrow{A_{IR}}(t')\right)^2 - E_A\right], \quad (5)$$

where E_A is the kinetic energy of the Auger electron in the absence of the IR field. Note that this is of a similar form to equation (2); in fact, both equations (1) and (4) can be written in the form

$$W_{el}(\vec{k}) = C\left|\int_{-\infty}^{\infty} dt \exp\left[i\Phi_{el}(\vec{k},t)\right] G_{el}(t)\right|^2, \quad (6)$$

with

$$\Phi_{el}(\vec{k},t) = -\int_t^{\infty} dt' \left[\frac{1}{2}\left(\vec{k} - \overrightarrow{A_{IR}}(t')\right)^2 - E_{el}\right]. \quad (7)$$

In equations (6) and (7), the subscript el refers to the type of electrons being described – that is, either to photoelectrons ph or Auger electrons A. For the photoelectrons, the factor $G_{el}(t)$ is given by

$$G_{ph}(t) = D_{\vec{k}}\widetilde{\varepsilon_X(t)}. \quad (8)$$

Henceforth, we shall set the dipole matrix element to unity and assume a simple Gaussian form for the X-ray pulse. Therefore,

$$G_{ph}(t) \approx \exp\left[-\frac{(t-\rho)^2}{2\sigma^2}\right], \quad (9)$$

where ρ is the delay of the X-ray pulse with respect to the IR pulse, which varies stochastically from shot to shot. For the Auger case, the factor $G_A(t)$ is dependent on the autoionising Auger state and its decay linewidth Γ:

$$G_A(t) = \sqrt{\frac{\Gamma}{2\pi}} \exp\left(-\frac{\Gamma}{2}t\right) \int_{t_0}^{t} dt' \exp\left(\frac{\Gamma}{2}t'\right) \tilde{\varepsilon}_X(t'). \tag{10}$$

We will refer to the factors $G_{el}(t)$ as effective pulses. The square of the effective pulse is equal to the corresponding emission profile. The electrons' final momenta will depend upon the vector potential of the IR pulse, which is given by

$$A_{IR}(t) = A_0(t) \sin(\omega_{IR} t), \tag{11}$$

where $\omega_{IR} = \frac{2\pi}{T_{IR}}$ is the angular frequency and T_{IR} is the period of the laser pulse. $A_0(t)$ represents the amplitude of the IR pulse. For simplicity, we will assume that the IR pulse is much longer than both the XFEL pulse and Auger decay lifetime. The result of this assumption is that for a *single shot*, the amplitude of the electric field interacting with photo- and Auger electrons can be assumed to be identical. However, $A_0(t)$ does vary on a timescale comparable to the timing jitter between X-ray and laser pulses, with the result that electrons emitted in *different* shots will generally interact with a different streaking amplitude. In Supplementary Figure 1, examples of functions G_{ph}^2 and G_A^2 are shown.

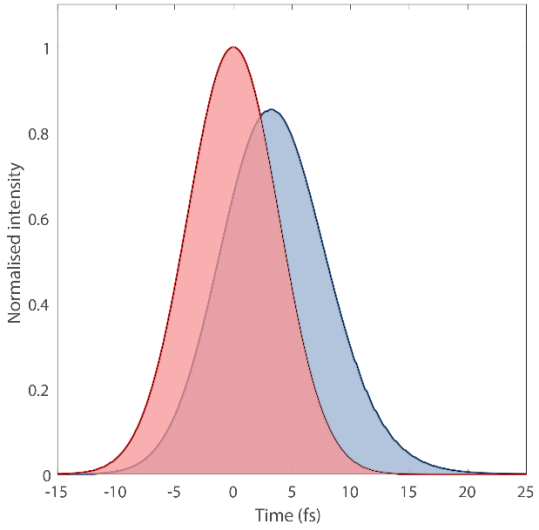

Supplementary Figure 1: Simulated photo- and Auger emission profiles| The red curve represents the photoemission profile, $G_{ph}^2(t)$, and the blue curve represents the Auger emission profile, $G_A^2(t)$. The time axis is relative to the time of arrival of the XFEL pulse. The delay between X-ray ionisation and the maximum of $G_A^2(t)$ is about 130 a.u. or 3.3 fs.

S2: Semiclassical approach

Whilst the final results presented in the main text were calculated using a fully quantum-mechanical approach, it is useful to first discuss a semiclassical approximation, which will be used to formulate a relationship between the final energy of an emitted electron and its moment of emission. The phase $\Phi(\vec{k}, t)$ in equation (7) varies rapidly in time, making direct computation of the state amplitudes time-consuming. However, the fast oscillation of the integrand in equation (6), which describes the probability of electron emission, means the result will be dominated by the saddle points, where the phase is stationary in time. These points t_s are defined by the condition $\frac{\partial \Phi(\vec{k},t)}{\partial t}|_{t=t_s} = 0$, with solutions given by

$$\left(\frac{k^2}{2} - E_{el}\right) - k\cos(\theta)\, A_{IR}(t_s) + \frac{A_{IR}^2(t_s)}{2} = 0, \tag{12}$$

where $k = |\vec{k}|$, $A_{IR}(t) = |\overrightarrow{A_{IR}}(t)|$, and θ is the angle of electron emission. Henceforth, we shall assume that the electrons are detected along the direction of polarisation of the pulses, so that $\theta = 0$. Equation (12) links the final momentum k, and hence final electron energy $E = \frac{k^2}{2}$, with the time of electron emission t_s. Solving it, we find

$$k - A_{IR}(t_s) = \sqrt{2E_{el}} = k_0; \qquad t_s = \frac{\arcsin\left[\frac{k-k_0}{A_0}\right]}{\omega_{IR}} + 2n\pi, \qquad n \in \mathbb{Z}, \tag{13}$$

where we have used the fact that for our experimental conditions, $A_0 \ll k, k_0$. In our experiment there is only one stationary point of Φ – the closest one to the excitation time τ – which contributes to the integrand in equation (6). Were the IR carrier frequency significantly higher, multiple stationary points would contribute, making the physical picture more complicated. This case is omitted from our discussion for brevity but could prove worthwhile for future investigation.

S3: Relationship between theoretical and experimentally measured quantities

In the experiment, time-of-flight (TOF) spectra for photoelectrons and Auger electrons are recorded for every shot. Each measurement is made with a different vector potential A_{IR}, because

neither the relative arrival time of the two pulses nor the carrier-envelope phase of the streaking pulse are controlled. This affects the shapes of the pair of TOF spectra obtained for each shot. After converting the spectra from TOF to kinetic energy, we evaluate the centre of energy (COE) for each of the two emission peaks. Plotting the laser-field-induced change in COE, ΔE, for each of the two peaks against one another results in the elliptical figure shown in the main text. Measuring the phase shift between this ellipse's parametric components is how we arrive at the time-delay between the two centres, and we will use this value to calculate the Auger decay lifetime.

Within the full quantum treatment of the experiment, we can compute the change in an emission peak's centre of energy due to interaction with the streaking laser:

$$\Delta E_{el} = \frac{\int \left(\frac{k^2}{2} - E_{el}\right) W_{el}(k)\, k\, dk}{\int W_{el}(k)\, k\, dk}. \tag{14}$$

Using the semiclassical approximation, we can transform the above expression and integrate over time instead of over emitted electron energy. Following the relations (13) and assuming that $A_{IR}(t) \ll k_0$, we find

$$\Delta E_{el} = k_0 \frac{\int A_{IR}(t) G_{el}^2(t) dt}{\int G_{el}^2(t) dt}. \tag{15}$$

It is straightforward to evaluate this expression for the photoelectrons; the photoemission profile $G_{ph}(t)$ is short compared to the period of the streaking pulse, since the XFEL pulse duration $\sigma \ll T_{IR}$. The result is that the streaking vector potential varies slowly compared to the timescale of photoemission, allowing us to obtain a simple approximation for the photoelectron case:

$$\Delta E_{ph} \approx k_0 A_{IR}(t_0) = A_0 \sqrt{2E_{ph}} \sin(\omega_{IR} t_0). \tag{16}$$

In this expression t_0 represents the arrival time of the XFEL pulse with respect to the streaking pulse. Note that equation (16) is equivalent to equation (3) from the main text.

The few-femtosecond Auger emission is also short compared to the period of the streaking pulse. Assuming a small variation in vector potential during Auger emission, one can expand $A_{IR}(t)$ about the XFEL arrival time t_0 using a Taylor series. Let the centre of time (COT) of the Auger emission profile be defined as

$$C_{TA} = \frac{\int t G_A^2(t) dt}{\int G_A^2(t) dt}. \tag{17}$$

Note that this quantity is independent of t_0. We can use this to obtain an approximate formula for ΔE_{Auger}:

$$\Delta E_{Auger} \approx k_0 A_{IR}(t_0 + C_{TA}) = A_0\sqrt{2E_A}\sin(\omega_{IR} t_0 + \phi), \tag{18}$$

where $\phi = \omega_{IR} C_{TA}$. This approximation provides a clear relation between the energy shift ΔE_{Auger} and the COT C_{TA} of the effective Auger pulse, and will enable us to relate the spectral-domain quantities measured in the experiment to the temporal properties of the decay process. In particular, comparing equations (16) and (18) shows us the time-delay between the COE of the photoemission and Auger streaked spectra is given by

$$\tau_{delay} = \frac{\phi T}{2\pi} = C_{TA} \tag{19}$$

S4: The phenomenological approach

It is worth comparing the quantum-mechanical theory described above with the phenomenological *ad hoc* theory, based upon rate equations, which has been applied in the past [5]. The latter is based on a description of the Auger process in terms of the following rate equation for the resonant Auger state population:

$$\frac{dn(t)}{dt} = -\kappa n(t) + S(t), \tag{20}$$

with solution

$$n(t) = \int_{-\infty}^{t} dt' \exp\big(-\kappa(t - t')\big) S(t') \,. \tag{21}$$

In equations (21) and (22), $n(t)$ represents the population of the Auger state, and $S(t)$ is a source term, usually defined as the probability of photoexcitation. The decay rate κ is related to the Auger decay lifetime τ_A according to the relation $\kappa = \frac{1}{\tau_A}$. The time-evolution of $n(t)$ characterises the Auger emission profile; thus, in the *ad hoc* model, when the core-excited state is induced by a Gaussian X-ray pulse of r.m.s. duration σ and the form

$$S(t') = \exp\left(-\frac{(t')^2}{\sigma^2}\right), \tag{22}$$

the temporal profile of the Auger emission will be given by

$$n(t) = \int_{-\infty}^{t} dt' \exp\left(-\frac{t'^2}{\sigma^2} - \kappa(t - t')\right). \tag{23}$$

In the preceding two equations, the zero of time is defined as the moment of interaction between the X-ray pulse and the target. Using this expression, we can show that this model predicts that the time-delay between the photo- and Auger emission bursts – the quantity τ_{delay} that we measured in our experiment – is identical to the Auger decay lifetime.

Note that, since the photoelectrons are emitted promptly upon interaction with the XFEL pulse, τ_{delay} is equivalent to the centre of mass of $n(t)$ in the time domain, given by

$$\tau_{delay} = \frac{\int_{-\infty}^{\infty} tA(t)dt}{\int_{-\infty}^{\infty} A(t)dt} = \frac{A_1}{A_0}. \tag{24}$$

First examine the denominator in equation (24):

$$\begin{aligned} A_0 &= \int_{-\infty}^{\infty} dt \int_{-\infty}^{t} \exp\left(-\frac{t'^2}{\sigma^2} - \kappa[t - t']\right) dt' \\ &= \int_{-\infty}^{\infty} dt \exp(-\kappa t) \int_{-\infty}^{t} \exp\left(-\frac{t'^2}{\sigma^2} + \kappa t'\right) dt'. \end{aligned} \tag{25}$$

Now, express $\exp(-\kappa t)$ as $-\frac{1}{\kappa}\frac{d\exp(-\kappa t)}{dt}$:

$$A_0 = -\frac{1}{\kappa}\int_{-\infty}^{\infty} dt \, \frac{d\exp(-\kappa t)}{dt} \int_{-\infty}^{t} \exp\left(-\frac{t'^2}{\sigma^2} + \kappa t'\right) dt'. \tag{26}$$

The next step is to integrate by parts:

$$A_0 = -\tau_A \left(\left[\exp(-\kappa t) \int_{-\infty}^{t} \exp\left(-\frac{t'^2}{\sigma^2} + \kappa t' \right) dt' \right]_{t=-\infty}^{\infty} - \int_{-\infty}^{\infty} dt \exp(-\kappa t) \frac{d}{dt} \left\{ \int_{-\infty}^{t} \exp\left(-\frac{t'^2}{\sigma^2} + \kappa t' \right) dt' \right\} \right)$$
$$= \tau_A \left(\int_{-\infty}^{\infty} dt \exp(-\kappa t) \exp\left(-\frac{t^2}{\sigma^2} + \kappa t \right) \right). \quad (27)$$

$$\therefore A_0 = \tau_A \int_{-\infty}^{\infty} dt \exp\left(-\frac{t^2}{\sigma^2} \right), \quad (28)$$

where we have noted that the term in the square brackets vanishes, and substituted $\tau_A = \frac{1}{\kappa}$. We can follow a similar procedure to evaluate the numerator in equation (24).

$$A_1 = \int_{-\infty}^{\infty} t \, dt \int_{-\infty}^{t} \exp\left(-\frac{t'^2}{\sigma^2} - \kappa[t - t'] \right) dt'$$
$$= \int_{-\infty}^{\infty} t \cdot \exp(-\kappa t) \, dt \int_{-\infty}^{t} \exp\left(-\frac{t'^2}{\sigma^2} + \kappa t' \right) dt'. \quad (29)$$

Expressing $t \cdot \exp(-\kappa t)$ as $-\frac{\partial}{\partial \kappa}\{\exp(-\kappa t)\}$, we can write A_1as follows:

$$A_1 = \int_{-\infty}^{\infty} -\frac{\partial}{\partial \kappa}\{\exp(-\kappa t)\} \, dt \int_{-\infty}^{t} \exp\left(-\frac{t'^2}{\sigma^2} + \kappa t' \right) dt'. \quad (30)$$

This equation now has a similar form to that of A_0 in equation (25) above. Adopting the same strategy before integrating by parts, we find

$$A_1 = \int_{-\infty}^{\infty} dt \, \frac{\partial}{\partial \kappa} \left\{ \frac{1}{\kappa} \frac{d \exp(-\kappa t)}{dt} \right\} \int_{-\infty}^{t} \exp\left(-\frac{t'^2}{\sigma^2} + \kappa t' \right) dt'$$
$$= \left(\left[\frac{\partial}{\partial \kappa} \left\{ \frac{1}{\kappa} \exp(-\kappa t) \right\} \int_{-\infty}^{t} \exp\left(-\frac{t'^2}{\sigma^2} + \kappa t' \right) dt' \right]_{t=-\infty}^{\infty} \right.$$
$$\left. - \int_{-\infty}^{\infty} dt \frac{\partial}{\partial \kappa} \left\{ \frac{1}{\kappa} \exp(-\kappa t) \right\} \cdot \frac{d}{dt} \left\{ \int_{-\infty}^{t} \exp\left(-\frac{t'^2}{\sigma^2} + \kappa t' \right) dt' \right\} \right) \quad (31)$$

$$A_1 = -\left(\int_{-\infty}^{\infty} dt \frac{\partial}{\partial \kappa}\left\{\frac{1}{\kappa}\exp(-\kappa t)\right\} \cdot \exp\left(-\frac{t^2}{\sigma^2} + \kappa t\right)\right), \tag{32}$$

again because the term in the square brackets vanishes. Evaluating the partial differential yields the following expression:

$$\begin{aligned} A_1 &= -\left(\int_{-\infty}^{\infty} dt \left(\frac{-1}{\kappa^2}\exp(-\kappa t) - t \cdot \exp(-\kappa t)\right) \exp\left(-\frac{t^2}{\sigma^2} + \kappa t\right)\right) \\ &= \int_{-\infty}^{\infty} dt \left(\frac{1}{\kappa^2} + t\right) \exp\left(-\frac{t^2}{\sigma^2} + \kappa t\right) \exp(-\kappa t) \\ &= \int_{-\infty}^{\infty} dt\, \tau_A^2 \exp\left(-\frac{t^2}{\sigma^2}\right) + \int_{-\infty}^{\infty} dt\, t \cdot \exp\left(-\frac{t^2}{\sigma^2}\right). \end{aligned} \tag{33}$$

The second term is zero, so finally,

$$A_1 = \tau_A^2 \int_{-\infty}^{\infty} dt \exp\left(-\frac{t^2}{\sigma^2}\right). \tag{34}$$

Now, we can complete the proof by combining equations (24), (28) and (34):

$$T = \frac{A_1}{A_0} = \frac{\tau_A^2 \int_{-\infty}^{\infty} dt \exp\left(-\frac{t^2}{\sigma^2}\right)}{\tau_A \int_{-\infty}^{\infty} dt \exp\left(-\frac{t^2}{\sigma^2}\right)} = \tau_A. \tag{35}$$

In summary, the Auger decay lifetime τ_A, which is defined as the reciprocal of the decay rate κ, has been shown to be identical to the centre of mass T of the temporal Auger emission profile – provided that we assume a probabilistic decay based upon the rate equation (20). Since the photoelectrons are emitted promptly after interaction with the XFEL pulse, T is also identical to the temporal displacement between the centres of mass of the two emission bursts τ_{delay}, which is the quantity measured in our experiment.

The *ad hoc* model uses the population of the continuum Auger states as its dynamical quantity, whilst the quantum model uses these states' amplitudes. In the quantum model, the population of the state is computed by integrating the amplitude of the states over time and squaring

the result. This difference in treatment means that the results predicted by the two models will generally differ, as discussed in the main text. However, in the limit of a very prompt excitation of the resonant state, both models predict an exponential decay in this state's population and will give similar results.

References:

1. Keldysh L.V. Ionization in the field of a strong electromagnetic wave. *Soviet Physics JETP* **20**, 1307 (1965).
2. Kazansky, A. K., Sazhina, I. P. & Kabachnik, N. M. Angle-resolved electron spectra in short-pulse two-color XUV+IR photoionization of atoms. *Phys. Rev. A* **82**, 033420 (2010).
3. Wolkow, D. M. Über eine Klasse von Lösungen der Diracschen Gleichung *Zeitschrift für Physik* **94**, 250 (1935).
4. Kazansky, A. K., Sazhina, I. P. & Kabachnik N. M. Time-dependent theory of Auger decay induced by ultra-short pulses in a strong laser field. *J. Phys. B* **42**, 245601 (2009).
5. Drescher, M. *et al.* Time-resolved atomic inner-shell spectroscopy, *Nature* **419** 803 (2002).